



[¹⁸F] AIF-NOTA-FAPI-04 PET/CT can predict treatment response and survival in patients receiving chemotherapy for inoperable pancreatic ductal adenocarcinoma

Ziyuan Zhu^{1,2} · Kai Cheng^{2,3} · Zhang Yun² · Xiang Zhang² · Xiaoyu Hu² · Jing Liu² · Fuhao Wang¹ · Zheng Fu^{2,3} · Jinbo Yue^{1,2}

Received: 13 February 2023 / Accepted: 18 May 2023 / Published online: 17 June 2023
© The Author(s), under exclusive licence to Springer-Verlag GmbH Germany, part of Springer Nature 2023

Abstract

Purpose We investigated whether uptake of [¹⁸F] AIF-NOTA-FAPI-04 on positron emission tomography/computed tomography (PET/CT) could predict treatment response and survival in patients with pancreatic ductal adenocarcinoma (PDAC). **Methods** We prospectively evaluated 47 patients with histopathologically confirmed primary PDAC who provided pre-treatment [¹⁸F] AIF-NOTA-FAPI-04 scans to detect fibroblast activation protein (FAP) on the tumor surface by uptake of [¹⁸F] AIF-NOTA-FAPI-04. PDAC specimens were immunohistochemically stained with cancer-associated fibroblast (CAF) markers. We obtained a second PET scan after one cycle of chemotherapy to study changes in FAPI uptake variables from before to during treatment. Correlations between baseline PET variables and CAF-related immunohistochemical markers were assessed with Spearman's rank test. Cox regression and Kaplan–Meier methods were used to assess relationships between disease progression and potential predictors. Receiver operating characteristic (ROC) curve analysis was used to define the optimal cut-off points for distinguishing patients according to good response vs. poor response per RECIST v.1.1.

Results The FAPI PET variables maximum and mean standardized uptake values (SUV_{max} , SUV_{mean}), metabolic tumor volume (MTV), and total lesion FAP expression (TLF) were positively correlated with CAF markers (FAP, α -smooth muscle actin, vimentin, S100A4, and platelet-derived growth factor receptor α/β , all $P < 0.05$). MTV was associated with survival in patients with inoperable PDAC (all $P < 0.05$). Cox multivariate regression showed that MTV was associated with overall survival (MTV hazard ratio [HR] = 1.016, $P = 0.016$). Greater changes from before to during chemotherapy in SUV_{max} , MTV, and TLF were associated with good treatment response (all $P < 0.05$). ΔMTV , ΔTLF , and ΔSUV_{max} had larger areas under the curve than $\Delta CA19-9$ for predicting treatment response. Kaplan–Meier analysis showed that the extent of change in MTV and TLF from before to after treatment predicted progression-free survival, with cut-off values (based on medians) of -4.95 for ΔMTV (HR = 8.09, $P = 0.013$) and -77.83 for ΔTLF (HR = 4.62, $P = 0.012$).

Conclusions A higher baseline MTV on [¹⁸F] AIF-NOTA-FAPI-04 scans was associated with poorer survival in patients with inoperable PDAC. ΔMTV was more sensitive for predicting response than $\Delta CA19-9$. These results are clinically meaningful for identifying patients with PDAC who are at high risk of disease progression.

Keywords Fibroblast activation protein · Pancreatic adenocarcinoma · Metabolic tumor volume · Total lesion FAP expression

Ziyuan Zhu and Kai Cheng made equal contributions to this work

✉ Zheng Fu
abbaab77@aliyun.com

✉ Jinbo Yue
jbyue@sdfmu.edu.cn

Extended author information available on the last page of the article

Introduction

Pancreatic cancer is one of the most aggressive and fatal types of cancer; the major histological subtype, pancreatic ductal adenocarcinoma (PDAC), accounts for 90% of all pancreatic cancer cases [1, 2]. One challenge in managing PDAC involves how best to assess the effectiveness of ongoing treatment.

Several studies found that a decrease in the tumor marker carbohydrate antigen (CA) 19–9 can be used to monitor response to chemotherapy and survival in patients with inoperable PDAC [3–5]. However, serum CA19-9 levels are elevated in only about 80% of patients with PDAC [6]. Interpretation and application of CA19-9 levels in PDAC are further complicated by their being affected by chronic pancreatitis, cholestasis, extrapancreatic malignancies, and lack of change despite the presence of malignancy [7, 8]. [¹⁸F]-fluorodeoxyglucose (FDG) PET/CT and PET/MR imaging can be useful for identifying local progression and metastatic spread and for evaluating response to treatment; however, their sensitivity for detecting PDAC is low [9]. [¹⁸F]-FDG is a nonspecific imaging agent with high uptake by both tumors and inflamed tissues; its relatively high background activity and uptake in normal organs may mask the presence of other lesions [10, 11]. New imaging agents with higher diagnostic and predictive efficiency are urgently needed.

Cancer-associated fibroblasts (CAFs) are major components of stromal cells that surround cancer cells, which have important roles in tumor proliferation, invasion, and metastasis and have been shown to enhance immune resistance [12]. Fibroblast activation protein (FAP) is a dipeptidyl peptidase 4 protein that has both endopeptidase and dipeptidyl peptidase activities [13]. It is highly expressed by more than 90% of epithelial tumors but is expressed at low levels in physiological conditions [14, 15]. FAP is expressed on the surface of CAFs and can regulate the structure and composition of the extracellular matrix and contribute to some tumor-promoting activities [16, 17]. FAP inhibitors (FAPIs) that specifically bind with FAP, linked with chelators and radionuclides, have been used in PET to reflect the biological distribution of FAP [18, 19]. Because FAP is expressed on the surfaces of CAFs, FAP inhibitors can be used to visualize CAF [20]. In one example, [⁶⁸Ga]-FAPI PET/CT was shown to have high sensitivity and specificity for the diagnosis and staging of PDAC.

In this study, we used PET/CT scanning with [¹⁸F] AIF-NOTA-FAPI-04 (in which NOTA-FAPI-04 was combined with AlCl₃ and radiolabeled with ¹⁸F), which has been confirmed safe and highly specific for FAP imaging [21], to explore whether uptake of [¹⁸F] AIF-NOTA-FAPI-04 on PET/CT could be used as a biomarker of response to therapy and survival in patients with inoperable PDAC. We reasoned that imaging that can detect or predict response to therapy could be useful for early intervention strategies to limit the progression and extent of disease. In the current study, we obtained FAPI PET/CT scans once before treatment and once during treatment through a prospective clinical protocol and correlated the findings with patient survival. We also determined the potential value of changes in FAPI PET variables from before to during chemotherapy for predicting response to chemotherapy.

Methods

Patients

This study was designed and implemented in Shandong Cancer Hospital from June 2021 to August 2022. The selection criteria were as follows: (1) histologically confirmed PDAC; (2) age ≥ 18 years; (3) good performance status (i.e., Eastern Cooperative Oncology Group score of 0–1); and (4) willingness to participate. The exclusion criteria were as follows: (1) not having an [¹⁸F] AIF-NOTA-FAPI-04 PET/CT scan before treatment and (2) history of other malignant disease within the past 5 years. We obtained an [¹⁸F] AIF-NOTA-FAPI-04 PET/CT scan from patients with inoperable pancreatic cancer before treatment, and we obtained a second PET scan after one cycle of chemotherapy to study changes in FAPI uptake variables from before to during treatment. The patient flow diagram is shown in Fig. 1.

This study was approved by the local institutional review board, and all patients who underwent [¹⁸F] AIF-NOTA-FAPI-04 PET/CT scanning provided written informed consent. Any patients who could not understand the study intent, had major psychiatric illness, or declined to participate were excluded from the study.

[¹⁸F] AIF-NOTA-FAPI-04 scanning

The radiotracer was synthesized as described previously [21]. Neither fasting nor blood glucose measurements were required before imaging. Patients were given an intravenous injection of 4.81 MBq/kg (0.12 mCi/kg) [¹⁸F] AIF-NOTA-FAPI-04 and instructed to rest for about 60 min before being scanned with a dedicated PET/CT system (GEMINI TF Big Bore; Philips Healthcare, Cleveland, OH, USA). Whole-body CT scans were obtained with attenuation correction by using a low-dose scanning protocol (300 mAs, 120 kV, a 512 × 512 matrix, rotation time of 1.0 s, and pitch index of 0.688; reconstructed with a soft-tissue kernel to a slice thickness of 2 mm). Subsequent PET scans were collected in 3D mode with a 200 × 200 matrix, and images were acquired in 1-min increments per bed position. Patients were instructed to breathe calmly during image acquisition. Attenuation-corrected PET data were reconstructed by using Body-tac-SB. LstcIn, Biograph 3D iterative reconstruction software with time-of-flight correction.

Imaging analysis

FAPI PET/CT images were obtained from patients once before treatment and again after one cycle of chemotherapy. Attenuation-corrected PET images, CT images, and fused PET/CT images were viewed and analyzed on MIM Maestro

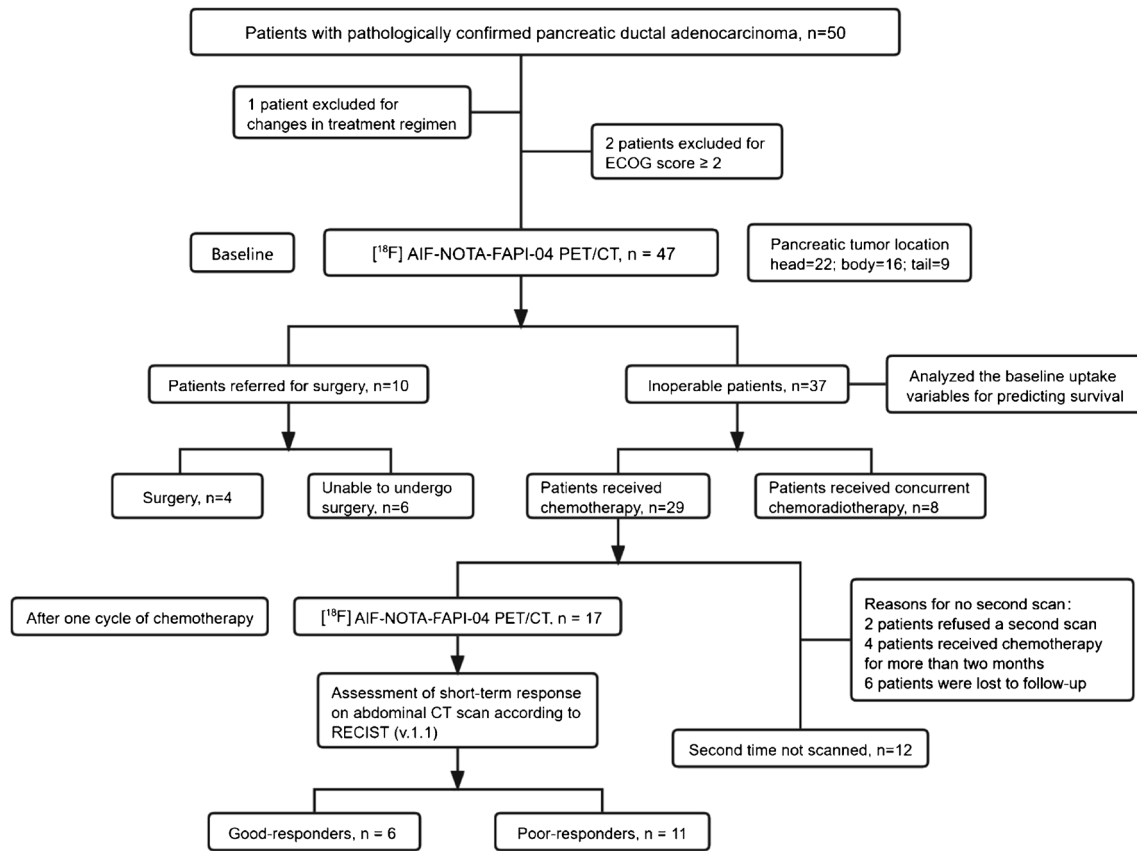


Fig. 1 CONSORT diagram

6.8.8 (MIM Software, Cleveland, OH), with images reconstructed in the coronal, sagittal, and transaxial planes. Two nuclear medicine physicians (each with > 15 years of experience) visually assessed the [^{18}F] AIF-NOTA-FAPI-04 PET/CT images with reference to contrast-enhanced CT scans and reached consensus regarding the presence and location of primary and metastatic tumor, any controversial neoplastic lesions, and inflammation suggestive of distal obstructive pancreatitis. These two physicians manually delineated regions of interest (ROIs) around the primary PDAC tumor and systemic metastases that showed higher uptake on the fusion PET/CT scans. The metabolic tumor volume (MTV) was derived from these ROIs by using a fixed SUV threshold method, in which a 3D contour was drawn automatically around voxels with $\geq 30\%$ of the SUV_{max} [21, 22]. Variables describing the tumor and metastases were automatically generated from the PET/CT scans by MIM Software and consisted of the maximum and mean standard uptake values (SUV_{max} and SUV_{mean}), MTV, total lesion FAP expression (TLF) of the primary tumor and systemic metastases, and SUV_{mean} of the primary tumor (Cancer SUV_{mean}). TLF was calculated as the product of the SUV_{mean} of all the lesions and the MTV ($\text{TLF} = \text{SUV}_{\text{mean}} \times \text{MTV}$) [23]. Changes in SUV_{max} from before to after one cycle of chemotherapy were

expressed as $\Delta\text{SUV}_{\text{max}} = (\text{SUV}_{\text{max}}$ after the first cycle minus the baseline SUV_{max}), and changes in other variables were calculated in the same way.

Two imaging specialists (each with > 15 years of experience) who were blinded to laboratory test results and follow-up records independently reviewed the contrast-enhanced CT images obtained at baseline and at 2 months after the first cycle of chemotherapy and recorded the location and size of the primary tumor in the axial plane. Responses were assessed according to RECIST v.1.1 on abdominal enhanced CT scans. Responses were characterized as complete response (CR), partial response (PR), stable disease (SD), and progressive disease (PD). Patients with CR or PR were classified as good responders, and patients with SD or PD as poor responders.

Clinical variables analysis

At the time of diagnosis (baseline) and after one cycle of chemotherapy (consistent with PET/CT scan times), peripheral blood samples were collected and analyzed for CA19-9, carcinoembryonic antigen (CEA), and neutrophil to lymphocyte ratio (NLR). Potential correlations between

these baseline clinical variables and progression-free survival (PFS) and overall survival (OS) were assessed. Changes in clinical variables from before to during treatment were also compared with the FAPI uptake variables, with response to therapy, and with survival. Therapy response was defined as CR, PR, SD, or PD according to RECIST v.1.1. OS was defined as the interval between the date of therapy and death or the last follow-up. PFS was defined as the interval between the date of therapy and tumor progression or the last follow-up.

Immunohistochemical analyses

Tissue samples (4 surgical specimens and 26 puncture [core] biopsies) were stained for immunohistochemical analysis by conventional methods as follows. Tissues were fixed in formalin, dehydrated, embedded in paraffin, cut into 5- μ m thick sections (Microm HM 450; GMI, Ramsey, MN, USA), and placed on glass slides. Staining with antibodies to FAP (R&D Systems, Q12884, 1:200 dilution), alpha smooth muscle actin (α -SMA; ServiceBio, GB13044, 1:200 dilution), platelet-derived growth factor receptor (PDGFR) α/β (Abcam, ab32570, 1:200 dilution), vimentin (ServiceBio, GB11192, 1:500 dilution), and the calcium-binding protein S100A4 (ServiceBio, GB11397, 1:500 dilution) was done according to standard protocols. Representative areas were selected by a pathologist on a TissueFAXS multispectral tissue cytometer (TissueGnostics, Austria), and three multispectral images were intercepted with 20 \times resolution field of view. Semi-quantitative pathology scores were calculated as the percentage of stained cells (scores of 0 for 0% positive cells, 1 for 1–25% positive cells, 2 for 26–50% positive cells, 3 for 51–75% positive cells, and 4 for 76–100% positive cells) \times staining intensity (0, no staining; 1, weak staining; 2, moderate staining; and 3, strong staining).

Statistical analysis

Patient characteristics were evaluated with descriptive statistics. Correlations between baseline PET variables and CAF-related immunohistochemical markers were assessed with Spearman's rank test. Normally distributed measurement data were expressed as means \pm SD, and non-normally distributed data as medians (with 25th to 75th percentiles). Mann–Whitney *U* tests were used to compare differences in various [18 F] AIF-NOTA-FAPI-04 PET/CT variables between good responders and poor responders. Cox proportional hazards regression was used to analyze the relationship between [18 F] AIF-NOTA-FAPI-04 PET/CT uptake variables and PFS and OS. Kaplan–Meier analysis was used

to compare survival outcomes in different subgroups, and comparisons were made with log-rank tests. A receiver operating characteristic (ROC) curve analysis was used to determine the best cut-off points for candidate predictors such as SUV_{max} , SUV_{mean} , MTV, and TLF. Statistical analyses were done with IBM SPSS Statistics version 24.0 (IBM, Armonk, NY, USA) and Prism 8.0.1 (GraphPad, San Diego, CA, USA).

Results

Patient characteristics

From June 2021 to June 2022, 47 patients with a histologically confirmed diagnosis of PDAC (22 in the head, 16 in the body, and 9 in the tail of the pancreas) were prospectively enrolled in a protocol at Shandong Cancer Hospital and Research Institute and provided baseline [18 F] AIF-NOTA-FAPI-04 PET/CT scans (Fig. 1). Patient characteristics are shown in Table 1. Ten of those 47 patients were referred to surgery, and the other 37 with inoperable PDAC (i.e., those who had unresectable [cTNM stage II–IV] disease at baseline) provided scans at baseline for analysis. Of those 37 patients, 8 received concurrent chemoradiotherapy and 29 received only chemotherapy. Among those 29 patients, 17 provided a second [18 F] AIF-NOTA-FAPI-04 PET/CT scan after one cycle of chemotherapy; of those 17 patients, 6 patients were classified as good responders (i.e., had CR or PR) and 11 patients as poor responders (i.e., had SD or PD).

[18 F]-FAPI-04PET/CT uptake and CAF biomarkers

To investigate whether the biological distribution of [18 F] AIF-NOTA-FAPI-04 PET/CT reflects the expression of CAF-related markers in PDAC, we tested tumor tissues from 10 patients who were referred for surgery and 20 patients with inoperable disease. A [18 F] AIF-NOTA-FAPI-04 PET/CT image of a patient with high FAPI uptake in the pancreas and physiological uptake levels in the gallbladder, bile ducts, and bladder is shown in Fig. 2a. Regarding the immunohistochemical staining results, FAP staining was observed in both the cell membrane and cytoplasm of tumor specimens, and staining for α -SMA, PDGFR α/β , vimentin, and S100A4 was observed in the cytoplasm (Fig. 2b). Spearman's rho showed that FAP staining was positively correlated with [18 F] AIF-NOTA-FAPI-04 PET/CT uptake variables (SUV_{max} , Cancer SUV_{mean} , MTV, and TLF; *P* for all < 0.05) (Fig. 2c). Expressions of α -SMA, vimentin, PDGFR α/β , and S100A4 were also positively correlated with SUV_{max} , Cancer SUV_{mean} , MTV, and TLF (*P* for all < 0.05) (Fig. 2c).

Table 1 Patient characteristics

Characteristics	Number of cases (%)
Age, years	
> 60	22 (47)
≤ 60	25 (53)
Sex	
Male	27 (57)
Female	20 (43)
ECOG score	
0	31 (66)
1	16 (34)
Pancreatic tumor location	
Head	22 (47)
Body	16 (34)
Tail	9 (19)
cTNM stage	
II	3 (6)
III	24(51)
IV	20(43)
T status	
T1–2	17 (36)
T3	11 (23)
T4	19 (40)
N status	
N0	21 (45)
N1	16 (34)
N2	10 (21)
M status	
M0	27 (57)
M1	20 (43)
Non-surgical therapy*	
AG	21 (57)
FOLFIRINOX	8 (22)
Concurrent chemoradiotherapy	8 (22)

*Given to 37 patients with inoperable disease

Abbreviations: ECOG, Eastern Cooperative Oncology Group; AG, gemcitabine and albumin-bound paclitaxel; FOLFIRINOX, oxaliplatin, irinotecan, fluorouracil, and leucovorin

Baseline [¹⁸F] AIF-NOTA-FAPI-04 PET/CT uptake variables predict PFS and OS in patients with inoperable PDAC

We analyzed baseline [¹⁸F] AIF-NOTA-FAPI-04 PET/CT uptake variables in 37 patients with inoperable PDAC patients for their potential ability to predict survival. We used ROC curve analysis to identify cut-off values for variables that were the most sensitive for predicting OS before therapy. Those cut-off values were 31.92 for MTV (area-under-the-curve value [AUC]=0.699, $P=0.049$), 7.72

for LOG_2 TLF (AUC = 0.705, $P=0.042$), and 3.52 for NLR (AUC = 0.715; $P=0.033$) (Fig. 3a).

In Cox univariate regression analysis, high MTV and high NLR were associated with higher risk of disease progression (P for both < 0.05), and high MTV, high LOG_2 TLF, and high NLR were associated with worse OS (P for all < 0.05) (Table 2). A correlogram showing significant positive correlations between MTV, LOG_2 TLF, and NLR is shown in Fig. 3b. In univariate analysis, four covariates with clinical impact (that is, age, sex, CA19-9 level, and cTNM) were not associated with PFS, but MTV was an independent predictor of PFS (hazard ratio [HR] = 1.011, 95% confidence interval [CI] 1.002–1.020, $P=0.015$, Fig. 3c). Because of the significant correlation between MTV and LOG_2 TLF (Spearman's correlation $r=0.883$, $P<0.001$), we only included MTV and clinical parameters (that is, age, sex, CA19-9 level, cTNM, and ECOG score) in the multivariate analysis. Finally, MTV was found to be an independent predictor of OS (MTV HR = 1.016, 95% CI 1.003–1.029, $P=0.016$) (Fig. 3d).

In ROC cut-off analyses for PFS and OS, having an MTV of > 50.10 was found to be associated with poor PFS (HR = 2.33, 95% CI 0.57–5.6, $P=0.032$) (Fig. 4a). As for OS, having an MTV value of > 31.92, a LOG_2 TLF value of > 7.72, and an NLR of > 3.53 were all associated with poor OS (MTV HR = 4.10, 95% CI 1.37–12.30, $P=0.045$, Fig. 4b; LOG_2 TLF HR = 4.06, 95% CI 1.36–12.12, $P=0.019$, Fig. 4c; and NLR HR = 4.27, 95% CI 1.00–18.34, $P=0.004$, Fig. 4d).

Changes in [¹⁸F] AIF-NOTA-FAPI-04 PET/CT variables can predict treatment response and PFS for patients with inoperable PDAC

We next explored whether changes in FAPI uptake variables from before to after one cycle of chemotherapy in 17 patients with inoperable PDAC could predict response to chemotherapy and survival. Representative CT and [¹⁸F] AIF-NOTA-FAPI-04 PET/CT imaging results for good responders and poor responders, classified according to RECIST (v.1.1), are shown in Fig. 5a. The extent of change (from baseline to during chemotherapy) in SUV_{max} , SUV_{mean} , MTV, TLF, and the clinical variables CA19-9, CEA, and NLR in good responders and poor responders are shown in Table 3. Greater changes in SUV_{max} , MTV, and TLF were noted in the good responders than in the poor responders (SUV_{max} , -3.63 ± 5.29 good vs. 2.16 ± 4.77 poor, $P=0.044$; MTV, -28.38 (-65.30 to -14.74) good vs. 2.38 (-4.95 to 14.95) poor, $P=0.002$; TLF, -191.77 (-275.15 to -105.37) good vs. 7.68 (-77.83 to 150.69) poor, $P=0.005$, Table 3, Fig. 5b). The extent of change in other variables did not differ between good responders and poor responders.

ROC curves were generated to assess the predictive accuracy of changes in [¹⁸F] AIF-NOTA-FAPI-04 PET/CT

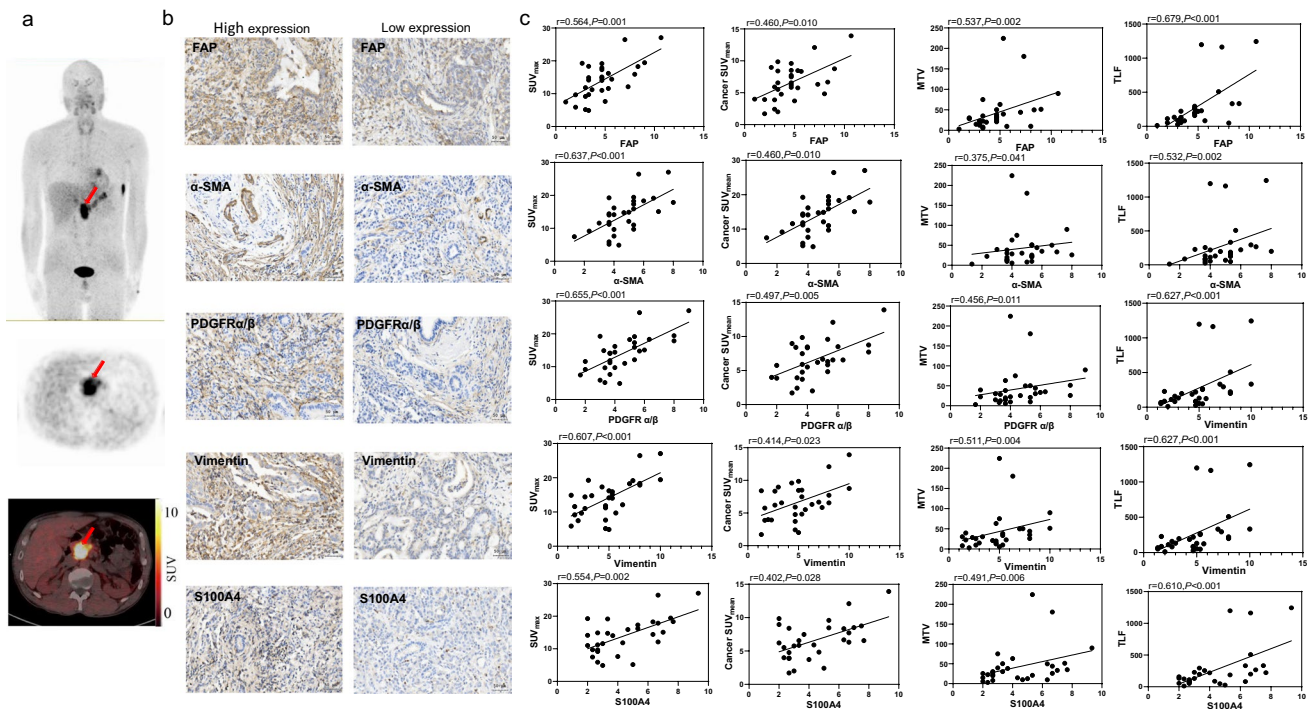


Fig. 2 **a** Representative [^{18}F] AIF-NOTA-FAPI-04 PET/CT scans of a patient with pancreatic adenocarcinoma; red arrows point to the pancreatic tumor. **b** Immunohistochemical stains of putative biomarkers of cancer-associated fibroblasts in representative tumor tissue sections, grouped as high expression (left) or low expression (right). FAP, fibroblast activation protein; α -SMA, α -smooth muscle actin; PDGFR, platelet-derived growth factor receptor; S100A4, calcium-

binding protein. **c** Correlations between measures of uptake of fibroblast activation protein inhibitor (FAPI; SUV_{max} , Cancer SUV_{mean} , MTV, and TLF) and immunohistochemical staining results for CAF-related markers (FAP, α -SMA, vimentin, PDGFR α/β , S100A4) in tumors. Significant correlations were found between FAPI uptake and expression of all 5 CAF-related biomarkers (P for all < 0.05)

variables for identifying good responders and poor responders. The ΔMTV AUC value (0.968; $P=0.002$) was higher than that for ΔTLF (AUC = 0.924, $P=0.005$) and $\Delta\text{SUV}_{\text{max}}$ (AUC = 0.803, $P=0.044$) (Table 4, Fig. 5c). The $\Delta\text{CA19-9}$ was smaller than these values and was not significant (AUC = 0.697, $P=0.191$). Kaplan–Meier analyses showed that good responders had better PFS (HR = 8.86, 95% CI 2.40–32.79, $P=0.007$) and OS (HR = NA, $P=0.0483$) than poor responders (Suppl. Figure 1a, b).

The extent of change in any [^{18}F] AIF-NOTA-FAPI-04 variable was not associated with the extent of change in the clinical variables CEA, CA19-9, or NLR (Fig. 6a). Cox univariate regression analysis showed that ΔMTV ($P=0.003$), ΔTLF ($P=0.008$), $\Delta\text{CA19-9}$ ($P=0.035$), and ΔNLR ($P=0.019$) were associated with PDAC disease progression (Table 5). Because ΔMTV had a significant positive correlation with ΔTLF , we included only ΔMTV , $\Delta\text{CA19-9}$, and ΔNLR in the multivariable analysis. Findings from that analysis showed that only ΔMTV ($P=0.02$) remained an independent predictor of PFS (Table 5, Fig. 6b). Finally, Kaplan–Meier analyses of PFS in patients grouped by median ΔMTV , ΔTLF , or $\Delta\text{CA19-9}$ values showed that ΔMTV and ΔTLF could distinguish good

from poor responders in terms of PFS (ΔMTV HR = 8.09, 95% CI 1.95–33.57, $P=0.013$; ΔTLF HR = 4.62, 95% CI 1.11–19.18, $P=0.012$, Fig. 6c), but $\Delta\text{CA19-9}$ could not.

Discussion

[^{18}F] AIF-NOTA-FAPI-04 PET/CT is expected to be an important reference method for monitoring response to treatment and assessing prognosis for patients with PDAC. In this study, we analyzed 37 patients with unresectable (cTNM stage II–IV) PDAC and found that having high MTV and TLF levels before therapy predicted poor survival. Further analysis of a second [^{18}F] AIF-NOTA-FAPI-04 PET/CT scan after one cycle of chemotherapy (obtained from 17 patients) revealed significant associations between changes in FAPI uptake variables among patients with good response to therapy according to RECIST (v.1.1). Our PET imaging data also allowed us to define cut-off values for extent of change in various FAPI uptake variables to distinguish patients with good response vs. those with poor response; specifically, ΔMTV

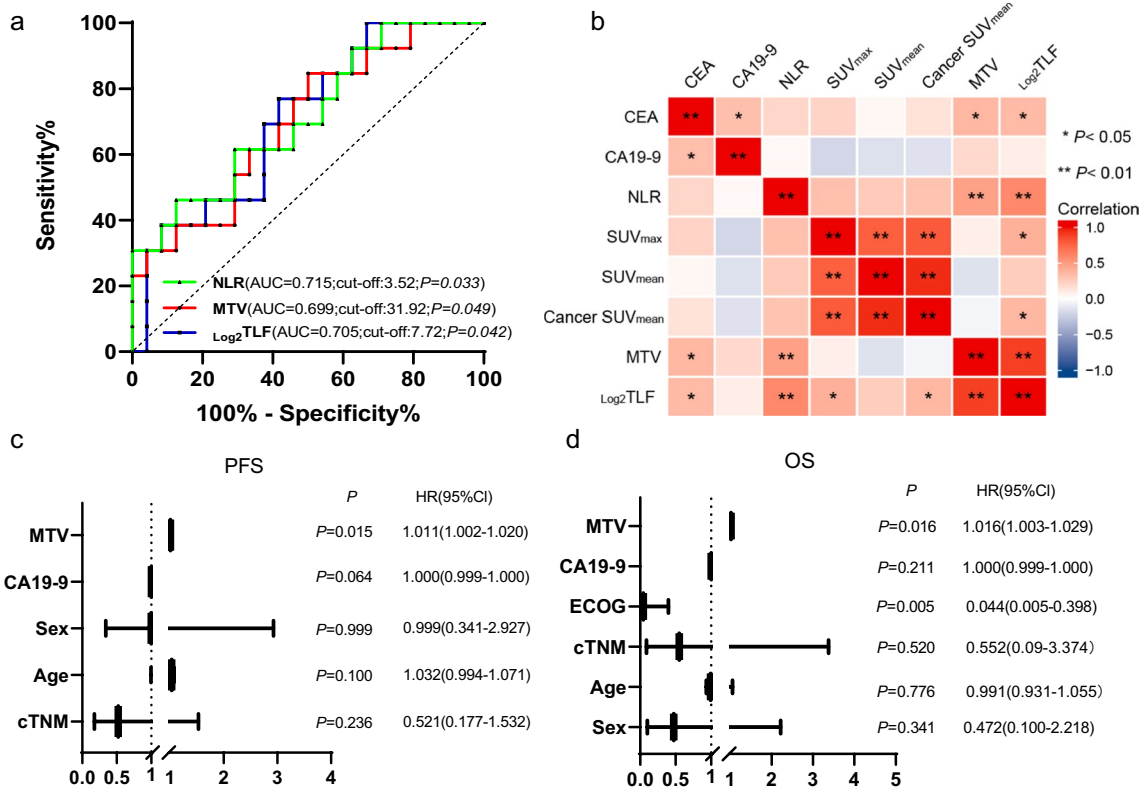


Fig. 3 **a** Correlogram showing Spearman correlation coefficients between [¹⁸F] AIF-NOTA-FAPI-04 PET/CT uptake variables and clinical or biological variables in patients with inoperable pancreatic ductal adenocarcinoma. Red indicates a positive correlation between two variables; blue, a negative correlation between two variables. Darker colors indicate stronger correlation. **b** Receiver operating characteristic curves for the ability of two [¹⁸F] AIF-NOTA-FAPI-04

PET/CT uptake values (MTV, LOG₂TLF) and NLR to predict overall survival (OS) in patients with inoperable pancreatic ductal adenocarcinoma. **c** Multivariate Cox regression analysis forest plot for progression-free survival (PFS). **d** Multivariate Cox regression analysis forest plot for OS. *P<0.05; **P<0.01. MTV, metabolic tumor volume; TLF, total lesion FAP expression; NLR, neutrophil-to-lymphocyte ratio

and ΔTLF were more sensitive than ΔCA19-9 for predicting treatment response. To the best of our knowledge, this is the first study to obtain serial FAPI PET scans before and after chemotherapy for PDAC and to correlate FAPI uptake variables with response to therapy.

In clinical practice, we have observed substantial variation between patients in the effectiveness of chemotherapy

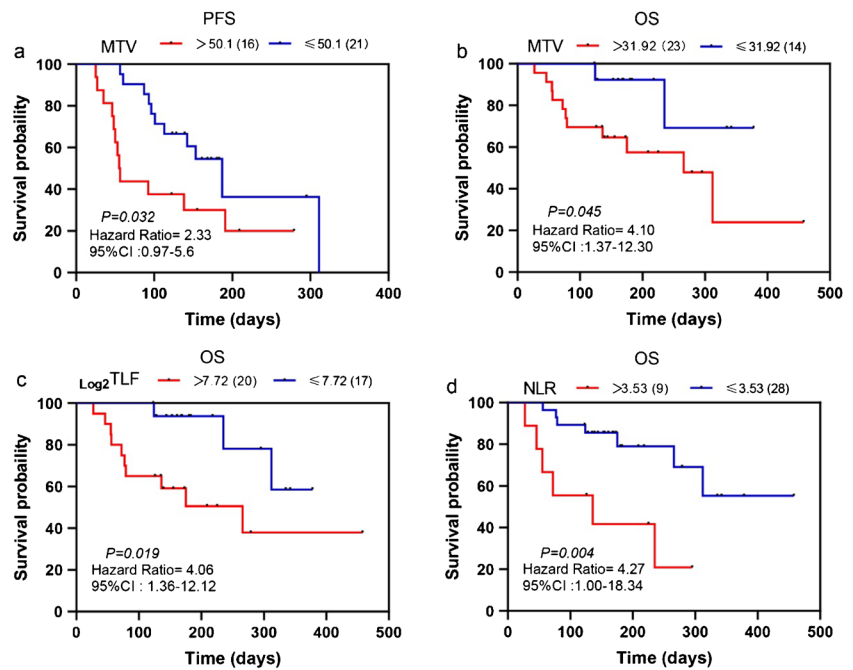
for PDAC, variations that could be related to the heterogeneity of the tumor microenvironment [24]. Therefore, monitoring the response to chemotherapy in individual patients is crucial for guiding early treatment decisions and offering prognostic information. The serum tumor marker CA19-9 is routinely used to monitor treatment response in clinical settings [3–5, 25]. However, limited numbers of patients in

Table 2 Univariate Cox regression analysis of variables associated with progression-free survival and overall survival

Variable	Progression-free survival			Overall survival		
	HR	95% CI	P value	HR	95% CI	P value
SUV _{max}	0.962	0.888–1.044	0.355	1.020	0.917–1.136	0.712
SUV _{mean}	0.948	0.795–1.130	0.550	1.100	0.887–1.363	0.386
MTV*	1.006	1.000–1.012	0.041	1.011	1.004–1.018	0.002
LOG ₂ TLF*	1.258	0.898–1.763	0.183	2.334	1.353–4.026	0.002
Cancer SUV _{mean}	0.940	0.787–1.122	0.493	1.110	0.894–1.377	0.344
CEA	0.983	0.947–1.021	0.376	0.995	0.966–1.025	0.733
CA19-9	1.000	1.000–1.000	0.512	1.000	0.999–1.000	0.545
NLR**	1.541	1.211–1.962	0.0001	2.177	1.460–3.246	0.0001

*P<0.05, **P<0.001

Fig. 4 a–d Progression-free survival (PFS) and overall survival (OS) analyses for patients with inoperable pancreatic ductal adenocarcinoma based on the indicated receiver operating characteristic curve cut-off values. MTV, metabolic tumor volume; TLF, total lesion FAP expression; NLR, neutrophil-to-lymphocyte ratio



reported studies, and variations in the definition of CA19-9 response among studies, have precluded identification of meaningful cut-off levels for response. Moreover, one retrospective analysis suggested that a decrease in serum CA19-9 levels during early-cycle chemotherapy was not associated with prolonged survival [26]. FAP is expressed mainly by stromal cells in the tumor microenvironment, where it promotes tumor cell invasion, migration, and tumor angiogenesis. Patients with tumors that express high levels of FAP seem to be at greater risk of developing drug resistance and poor prognosis [27, 28].

Several studies have shown that [⁶⁸Ga]-FAPI PET/CT is more sensitive than [¹⁸F]-FDG PET/CT for identifying abdominal lymph nodes, liver and bone metastases, and peritoneal cancer [29, 30]. We chose the nuclide ¹⁸F deliberately because of its longer half-life ($T_{1/2} = 109$ min, 97% β^+ , 0.64 MeV) and shorter β^+ trajectory (< 2 mm), which lead to excellent imaging resolution [31, 32]. Our results indicated that [¹⁸F] AIF-NOTA-FAPI-04 PET/CT biodistribution was significantly correlated with FAP expression in patients with PDAC. Mona et al. reported that FAP expression correlated with ⁶⁸Ga-FAPI-46 SUV_{max} and SUV_{mean} in several types of cancer [33], which is consistent with our results. FAPI uptake has also been reported to be moderately positively correlated with FAP expression in biopsy specimens ($r = 0.439$, $P = 0.012$) [21]. We also found here that FAPI uptake variables were moderately positively correlated with FAP, and we surmise that this modest correlation may result from tumor heterogeneity, tumor location, and biopsy location [34]. Wikberg et al. [35] observed heterogeneity in FAP expression in colorectal cancer with pathology

confirmation. Because immunochemical staining results are by definition affected by intratumoral heterogeneity and the limitations associated with biopsy sampling [36, 37], others have proposed that SUV_{mean} may better reflect FAP expression in the entire tumor [38, 39].

The mesenchymal origin of CAFs is manifested by their high expression of α -SMA, and PDGFR α/β in addition to FAP; indeed, overexpression of PDGFR α/β has been linked with poor prognosis in several types of cancer [40, 41]. Vimentin, an intermediate filament protein, is considered a marker of the epithelial-mesenchymal transition; cancer cells that express vimentin are more likely to invade and migrate [42]. S100A4 is located mostly in the cytoplasm, where it regulates cytoskeleton components and promotes the motility and invasion of tumor cells. S100A4 has also been shown to promote growth factor release, angiogenesis, and overall tumor survival [43, 44]. Given our finding that FAPI uptake variables were significantly correlated with these CAF-related markers, we explored whether [¹⁸F] AIF-NOTA-FAPI-04 PET/CT would be useful for predicting, before treatment has begun, treatment effectiveness and survival.

Because no consensus has been reached regarding the optimal SUV threshold for FAPI measurements, our ROIs were manually delineated on PET/CT fusion scans with reference to contrast-enhanced CT [45]. Although [¹⁸F]-FDG PET/CT variables have been used to predict prognosis in pancreatic cancer, which marker is the best for this purpose remains controversial [46, 47]. Another potential marker, NLR, is a surrogate for a systemic inflammatory response and can provide valuable prognostic information in many types of cancer, including that of the pancreas. At least one

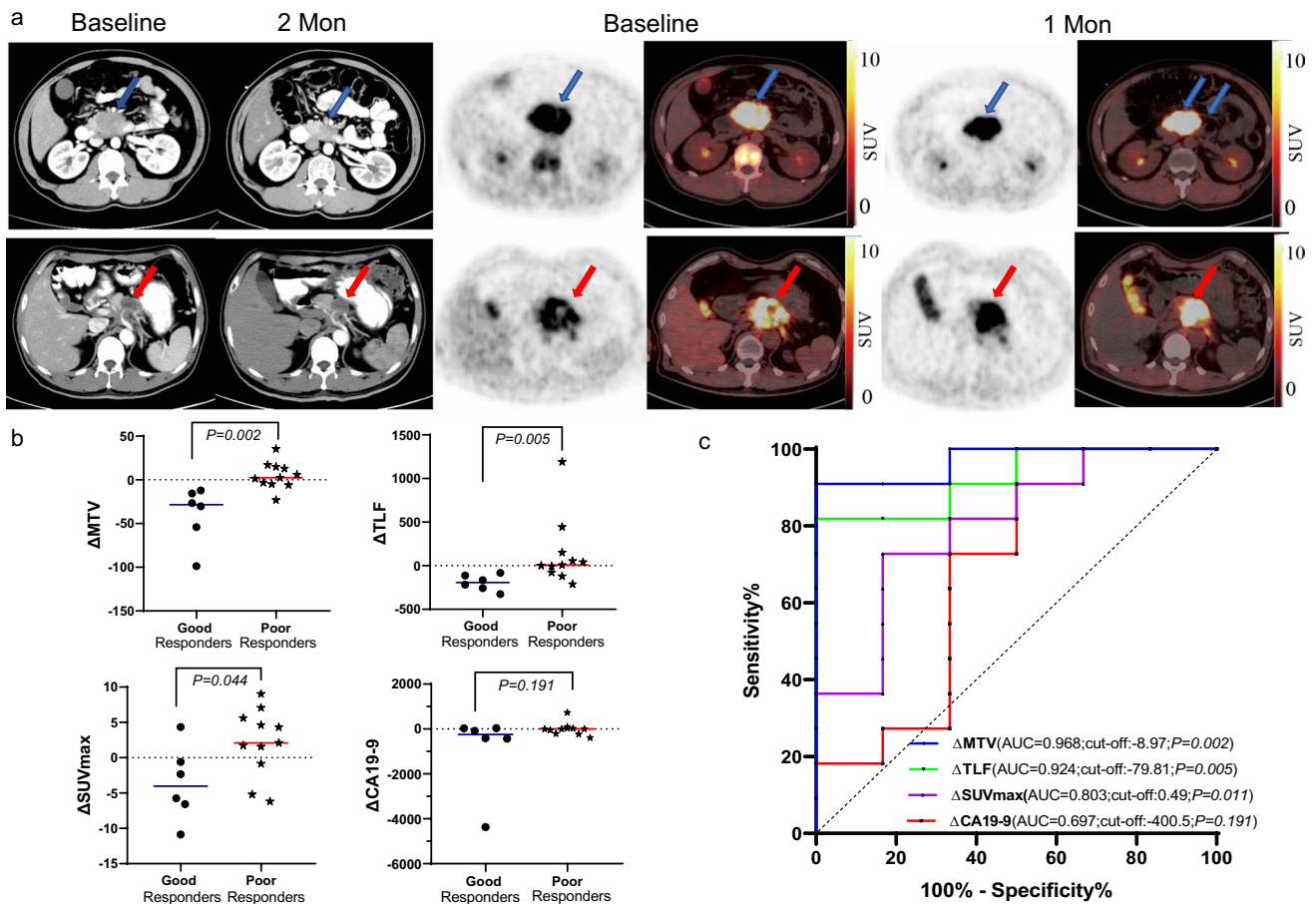


Fig. 5 a Representative $[^{18}\text{F}]$ AIF-NOTA-FAPI-04 PET/CT and CT images of inoperable pancreatic ductal adenocarcinoma in good responders (top row) and poor responders (bottom row). Blue arrows point to pancreatic tumor in good responders, red arrows to tumors in poor responders. **b** Extent of change (Δ) in PET/CT variables from baseline to after chemotherapy distinguishes good responders from poor responders to treatment for inoperable pancreatic ductal

adenocarcinoma. ΔMTV , change in metabolic tumor volume; ΔTLF , change in FAP expression in all lesions; $\Delta\text{SUV}_{\text{max}}$, change in maximum standardized uptake value; $\Delta\text{CA19-9}$, change in CA19-9 levels. **c** Receiver operating characteristic curve analyses of cut-off values for the extent of change in ΔMTV , ΔTLF , $\Delta\text{SUV}_{\text{max}}$, and CA19-9 and response to chemotherapy. * $P < 0.05$; ** $P < 0.01$

group has shown that patients with pancreatic cancer and high NLR have shorter survival times [48], a finding consistent with that of the current study. We also found that having higher baseline MTV and TLF were associated with poor OS. Although baseline TLF did not correlate with PFS in our Cox multivariable analysis, MTV was more strongly correlated with survival outcomes, perhaps because MTV is a better indicator of systemic metabolic tumor load. This variable may prove helpful in future studies for identifying patients at higher risk of disease progression before treatment, so that personalized therapy can be considered for such patients.

Another study conducted at the Shandong Cancer Hospital and Institute showed that findings on $[^{18}\text{F}]$ AIF-NOTA-FAPI-04 PET/CT were associated with short-term treatment response in patients with locally advanced esophageal squamous cell carcinoma [23]. Another study has shown that changes in the intensity of FAPI uptake on $[^{68}\text{Ga}]$ -FAPI-04

PET/CT can be used to objectively assess treatment effectiveness and perhaps to identify patients at higher risk of disease [49]. We found that the extent of change in CA19-9 (from before to during chemotherapy) could not distinguish good from poor responders, findings that agree with those from other studies that changes in CA19-9 (from before to after early cycle of chemotherapy) were not correlated with good response to therapy [50, 51]. Our own analysis of FAPI PET/CT variables before and during chemotherapy for PDAC showed that having lower FAPI uptake (indicated by SUV_{max} , MTV, and TLF) during chemotherapy was better able to distinguish good from poor responders than the extent of change in CA19-9 levels. Our results suggest that patients who show a good response early in the course of therapy have longer survival, which is consistent with clinical observations.

We were also able to define cut-off values for variables that predicted survival from the median values of those

Table 3 Changes in variables from baseline to after one cycle of chemotherapy for advanced pancreatic ductal adenocarcinoma

Variables	Poor responders (<i>n</i> = 11)			Good responders (<i>n</i> = 6)			<i>P</i> values		
	Before	After	Change	Before	After	Change	Before	After	Change
SUV _{max} *	12.88 ± 4.91	15.05 ± 5.87	2.16 ± 4.77	16.57 ± 3.80	12.95 ± 3.68	− 3.63 ± 5.29	0.097	0.546	0.044
SUV _{mean}	5.69 ± 2.51	5.60 ± 1.99	− 0.86 ± 2.90	5.87 ± 1.93	4.69 ± 1.57	− 1.18 ± 2.03	0.920	0.393	0.546
MTV*	20.90 (15.44–75.15)	26.76 (16.83–90.11)	2.38 (− 4.95 to 14.95)	65.23 (24.47–116.92)	33.33 (9.73–56.90)	− 28.38 (− 65.30 to − 14.74)	0.228	0.688	0.002
TLF*	145.53 (81.18–331.67)	119.97 (79.05–281.18)	7.68 (− 77.83 to 150.69)	364.51 (191.16–462.07)	126.86 (47.26–307.14)	− 191.77 (− 275.15 to − 105.37)	0.108	0.688	0.005
Cancer SUV _{mean}	6.19 ± 2.48	5.93 ± 2.86	− 0.26 ± 2.71	7.06 ± 1.63	5.44 ± 1.35	− 1.63 ± 1.87	0.546	0.688	0.269
CEA	1.49 (0.77–2.22)	1.62 (1.15–2.76)	0.41 (0.09–1.15)	7.79 (3.53–39.10)	7.71 (2.50–14.88)	− 0.75 (− 29.11 to 1.59)	0.006	0.031	0.065
CA19-9	139.00 (12.50–467.00)	71.70 (15.20–305.00)	0.88 (− 208.70 to 31.50)	629.50 (432.25–3063.25)	419.50 (277.50–1871.00)	− 246.5 (− 1414.25 to 30.50)	0.021	0.018	0.191
NLR	2.79 ± 2.23	2.27 (1.65–3.84)	0.39 (− 0.24 to 0.76)	2.56 ± 0.58	2.22 ± 0.79	− 0.33 ± 0.91	0.763	0.763	0.132

Δ, change from baseline to after chemotherapy; *NLR*, neutrophil–lymphocyte ratio. **P* < 0.05

variables; namely, a ΔMTV greater than − 4.95 and a ΔTLF greater than − 77.83 after treatment were useful for identifying patients at higher risk of disease progression—patients who could require more intensive disease management. In the current study, 8 patients received concurrent chemoradiotherapy, most of whom exhibited higher level of FAPI uptake after chemoradiotherapy. Possible indications of elevated SUV_{max} in some of these patients (data not shown) are being analyzed for future studies.

The major limitations of this current study are its single-center design and its relatively small number of patients, but our results are sound for the following reasons. Having a smaller

GTV_{FAPI} was previously found to be associated with significantly better PFS and OS [52], which is consistent with our results. The changes in [¹⁸F] AIF-NOTA-FAPI-04 uptake variables and clinical variables from before to during chemotherapy were reliable on re-analysis that included or excluded outliers (not shown) and are in line with clinical observations. Moreover, the nonparametric Mann–Whitney *U* test is well suited for analysis of small samples, is sensitive to differences in data distribution, and is relatively unaffected by outliers [53, 54], which is why we used this test to analyze differences in FAPI uptake and clinical variables between good responders and poor responders. Another limitation of our study is the heterogeneity

Table 4 Areas under the curve for changes in ¹⁸F-FAPI-PET/CT variables and extent of change in clinical variables (from baseline to after chemotherapy) for predicting response to chemotherapy for advanced pancreatic ductal adenocarcinoma

Variables	Area	SE [†]	Asymptotic Sig. [‡]	Asymptotic 95% confidence interval	
				Lower bound	Upper bound
ΔSUV _{max} *	0.803	0.114	0.044	0.579	1.000
ΔSUV _{mean}	0.591	0.141	0.546	0.315	0.867
ΔMTV*	0.968	0.038	0.002	0.896	1.000
ΔTLF*	0.924	0.064	0.005	0.798	1.000
ΔCancer SUV _{mean}	0.667	0.134	0.269	0.405	0.929
ΔCEA	0.783	0.141	0.065	0.507	1.000
ΔCA19-9	0.697	0.154	0.191	0.396	0.998
ΔNLR	0.727	0.138	0.132	0.456	0.998

[†]Null hypothesis: true area = 0.5

[‡]Under the nonparametric assumption

Δ, change in variable from baseline to after treatment

**P* < 0.05

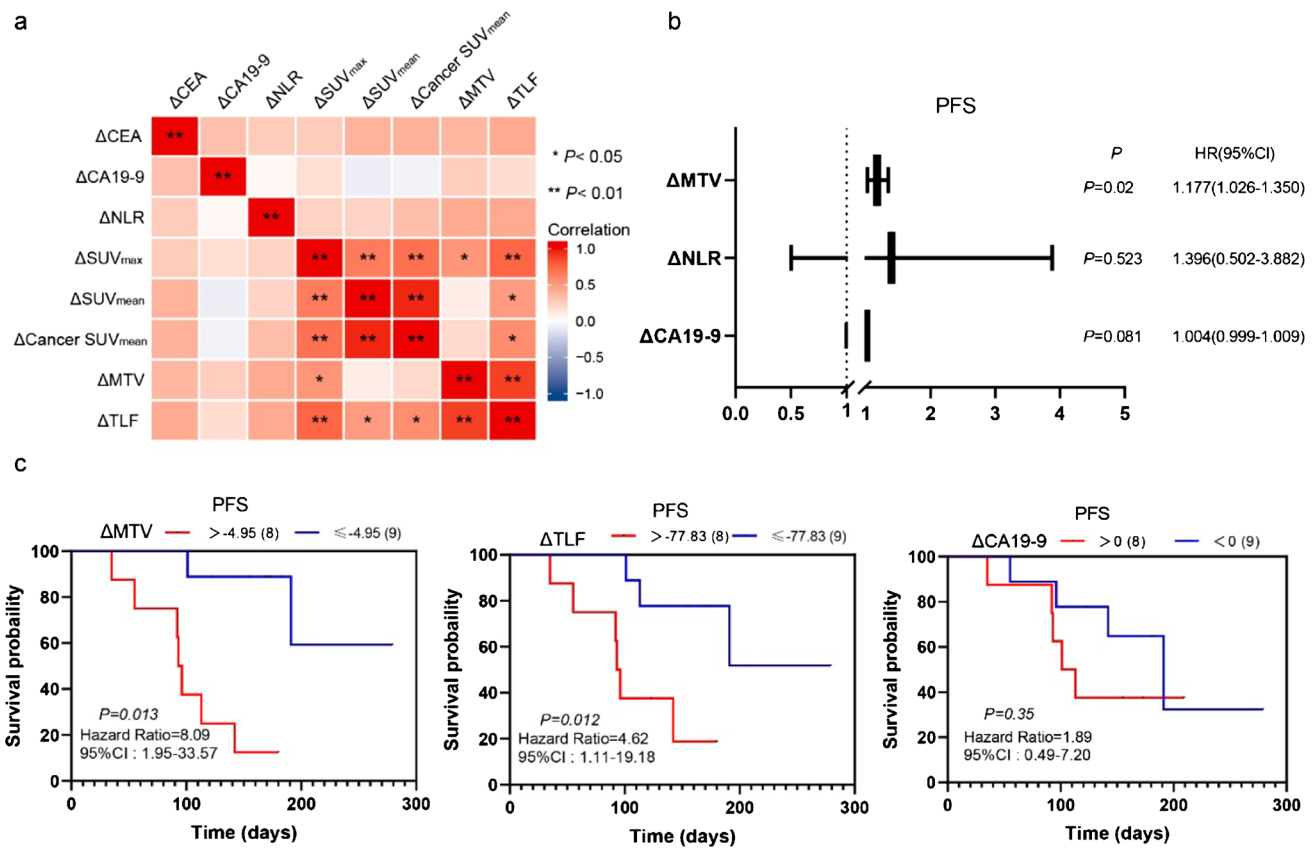


Fig. 6 **a** Correlogram shows Spearman correlation coefficients for extent of change in [¹⁸F] AIF-NOTA-FAPI-04 PET/CT variables and extent of changes in clinical variables. **b** Multivariate Cox regression forest plot of the extent of change in variables potentially associated with progression-free survival (PFS). Δ MTV, extent of change in metabolic tumor volume from before to after treatment; Δ TLF,

change in extent of total FAP expression in all lesions; Δ CA19-9, extent of change in CA19-9 levels in blood samples obtained before and after treatment. **c** Analysis of PFS based on cut-off values (above or below medians of the extent of change in metabolic tumor volume (MTV), total FAP expression in all lesions (TLF), and CA19-9 level

in chemotherapy regimens (AG vs. FOLFIRINOX), which may have influenced the outcomes. However, a large retrospective analysis of chemotherapy regimens used for advanced pancreatic cancer in China found no significant difference in disease control for patients given FOLFIRINOX and those given AG, and no differences in median PFS or OS times [55]. Finally,

MTV and TLF can be influenced by many confounding factors, including partial volume effects, image resolution, and time between tracer injection and imaging; nevertheless, our results suggest that they may be valuable for assessing tumor burden. Overall, further prospective trials are needed to confirm the utility of [¹⁸F] AIF-NOTA-FAPI-04 PET/CT in PDAC.

Table 5 Univariate and multivariate Cox regression analyses of changes in [¹⁸F]-FAPI-04 PET/CT variables and clinical variables

Factor	Univariate analysis		Multivariate analysis	
	HR (95% CI)	P value	HR (95% CI)	P value
Δ SUV _{max}	1.105 (0.961–1.272)	0.162	—	—
Δ SUV _{mean}	1.020 (0.760–1.369)	0.896	—	—
Δ MTV*	1.153 (1.049–1.269)	0.003	1.177 (1.026–1.350)	0.020
Δ TLF	1.010 (1.003–1.018)	0.008	—	—
Δ Cancer SUV _{mean}	1.043 (0.771–1.410)	0.785	—	—
Δ CEA	1.222 (0.992–1.506)	0.060	—	—
Δ CA19-9	1.003 (1.000–1.005)	0.035	1.004 (0.999–1.009)	0.081
Δ NLR	1.962 (1.119–3.442)	0.019	1.396 (0.502–3.882)	0.523

Δ , change in variable from baseline to after one round of chemotherapy, * $P < 0.05$

Conclusions

This study provided evidence to support the clinical significance of metabolic tumor burden measured by [¹⁸F] AIF-NOTA-FAPI-04 imaging. The baseline MTV was associated with the better PFS and OS in patients with PDAC. The extent of changes in FAPI uptake variables from before to after one cycle of chemotherapy for PDAC correlated significantly with response to treatment. The identified cut-off values or Δ MTV (> -4.95) and Δ TLF (> -77.83) may be clinically meaningful for identifying patients at high risk of disease progression. We conclude that findings from pretreatment [¹⁸F] AIF-NOTA-FAPI-04 scanning may be useful biomarkers of survival in patients with PDAC and can inform the identification of high-risk patients requiring aggressive intensive therapy.

Supplementary Information The online version contains supplementary material available at <https://doi.org/10.1007/s00259-023-06271-8>.

Acknowledgements We would like to thank the staff at PET/CT center, Shandong Cancer Hospital, for their contributions to tracer preparation and PET/CT imaging.

Author contribution Jinbo Yue conceived and designed the study. Ziyuan Zhu participated in the experimental design and conduct and drafted the manuscript. Kai Cheng was responsible for preparation of the [¹⁸F] AIF-NOTA-FAPI-04. Ziyuan Zhu and Jing Liu were responsible for collecting PET/CT images. Zheng Fu and Yun Zhang carried out the nuclear medicine. Zheng Fu and Jinbo Yue assessed responses on the images per the RECIST system (v.1.1). Xiang Zhang did the pathology analyses. Fuhao Wang was responsible for data analysis. All authors read and approved the final manuscript.

Funding This work was supported by the following grants: National Natural Science Foundation of China (82272753), Young TaiShan Scholars and Academic Promotion Program of Shandong First Medical University (2019RC003), Shandong Provincial Natural Science Foundation (ZR2021LZL002), Bethune Cancer Radiotherapy Translational Medicine Research Fund (flzh202103).

Data availability The datasets used or analyzed during the current study are available from the corresponding author on reasonable request.

Code availability All software applications or custom code are available in the public repository.

Declarations

Ethics approval and consent to participate This study was approved by the local ethics committee of Shandong Cancer Hospital and Institute, and the patient gave written and informed consent before the study.

Consent for publication All authors of the current manuscript meet the specified criteria for authorship and agreed to publish.

Conflict of interest The authors declare no competing interests.

References

1. Siegel RL, Miller KD, Wagle NS, Jemal A. Cancer statistics. *CA: Cancer J Clin.* 2023;73:17–48. <https://doi.org/10.3322/caac.21763>.
2. Rahib L, Wehner MR, Matrisian LM, Nead KT. Estimated projection of US cancer incidence and death to 2040. *JAMA Netw Open.* 2021;4:e214708. <https://doi.org/10.1001/jamanetworkopen.2021.4708>.
3. Ko AH, Hwang J, Venook AP, Abbruzzese JL, Bergsland EK, Tempero MA. Serum CA19-9 response as a surrogate for clinical outcome in patients receiving fixed-dose rate gemcitabine for advanced pancreatic cancer. *Br J Cancer.* 2005;93:195–9. <https://doi.org/10.1038/sj.bjc.6602687>.
4. Humphris JL, Chang DK, Johns AL, Scarlett CJ, Pajic M, Jones MD, et al. The prognostic and predictive value of serum CA19.9 in pancreatic cancer. *Ann Oncol.* 2012;23:1713–22. <https://doi.org/10.1093/annonc/mdr561>.
5. Maisey NR, Norman AR, Hill A, Massey A, Oates J, Cunningham D. CA19-9 as a prognostic factor in inoperable pancreatic cancer: the implication for clinical trials. *Br J Cancer.* 2005;93:740–3. <https://doi.org/10.1038/sj.bjc.6602760>.
6. Kondo N, Murakami Y, Uemura K, Hayashidani Y, Sudo T, Hashimoto Y, et al. Prognostic impact of perioperative serum CA 19–9 levels in patients with resectable pancreatic cancer. *Ann Surg Oncol.* 2010;17:2321–9. <https://doi.org/10.1245/s10434-010-1033-0>.
7. Dumitra S, Jamal MH, Aboukhalil J, Doi SA, Chaudhury P, Hassanain M, et al. Pancreatic cancer and predictors of survival: comparing the CA 19–9/bilirubin ratio with the McGill Brisbane Symptom Score. *HPB.* 2013;15:1002–9. <https://doi.org/10.1111/hpb.12085>.
8. La Greca G, Sofia M, Lombardo R, Latteri S, Ricotta A, Puleo S, et al. Adjusting CA19-9 values to predict malignancy in obstructive jaundice: influence of bilirubin and C-reactive protein. *World J Gastroenterol.* 2012;18:4150–5. <https://doi.org/10.3748/wjg.v18.i31.4150>.
9. Zhang L, Sanagapalli S, Stoita A. Challenges in diagnosis of pancreatic cancer. *World J Gastroenterol.* 2018;24:2047–60. <https://doi.org/10.3748/wjg.v24.i19.2047>.
10. Strobel O, Büchler MW. Pancreatic cancer: FDG-PET is not useful in early pancreatic cancer diagnosis. *Nat Rev Gastroenterol Hepatol.* 2013;10:203–5. <https://doi.org/10.1038/nrgastro.2013.42>.
11. Jha P, Bijan B. PET/CT for pancreatic malignancy: potential and pitfalls. *J Nucl Med Technol.* 2015;43:92–7. <https://doi.org/10.2967/jnmt.114.145458>.
12. Koustoulidou S, Hoorens MWH, Dalm SU, Mahajan S, Debets R, Seimbille Y, et al. Cancer-associated fibroblasts as players in cancer development and progression and their role in targeted radionuclide imaging and therapy. *Cancers.* 2021;13. <https://doi.org/10.3390/cancers13051100>.
13. de Sostoa J, Fajardo CA, Moreno R, Ramos MD, Farrera-Sal M, Alemany R. Targeting the tumor stroma with an oncolytic adenovirus secreting a fibroblast activation protein-targeted bispecific T-cell engager. *J Immunother Cancer.* 2019;7:19. <https://doi.org/10.1186/s40425-019-0505-4>.
14. Christiansen VJ, Jackson KW, Lee KN, Downs TD, McKee PA. Targeting inhibition of fibroblast activation protein- α and prolyl oligopeptidase activities on cells common to metastatic tumor microenvironments. *Neoplasia (New York, NY).* 2013;15:348–58. <https://doi.org/10.1593/neo.121850>.
15. Li Z, Sun C, Qin Z. Metabolic reprogramming of cancer-associated fibroblasts and its effect on cancer cell reprogramming. *Theranostics.* 2021;11:8322–36. <https://doi.org/10.7150/thno.62378>.
16. Šimková A, Bušek P, Šedo A, Konvalinka J. Molecular recognition of fibroblast activation protein for diagnostic and therapeutic

- applications. *Biochimica et Biophysica Acta Proteins and Proteomics*. 2020;1868:140409. <https://doi.org/10.1016/j.bbapap.2020.140409>.
17. Mazur A, Holthoff E, Vadali S, Kelly T, Post SR. Cleavage of type I collagen by fibroblast activation protein- α enhances class A scavenger receptor mediated macrophage adhesion. *PLoS one*. 2016;11:e0150287. <https://doi.org/10.1371/journal.pone.0150287>.
 18. Puré E, Blomberg R. Pro-tumorigenic roles of fibroblast activation protein in cancer: back to the basics. *Oncogene*. 2018;37:4343–57. <https://doi.org/10.1038/s41388-018-0275-3>.
 19. Hosein AN, Brekken RA, Maitra A. Pancreatic cancer stroma: an update on therapeutic targeting strategies. *Nat Rev Gastroenterol Hepatol*. 2020;17:487–505. <https://doi.org/10.1038/s41575-020-0300-1>.
 20. Liermann J, Syed M, Ben-Josef E, Schubert K, Schlampp I, Sprengel SD, et al. Impact of FAPI-PET/CT on target volume definition in radiation therapy of locally recurrent pancreatic cancer. *Cancers*. 2021;13. <https://doi.org/10.3390/cancers13040796>.
 21. Wei Y, Cheng K, Fu Z, Zheng J, Mu Z, Zhao C, et al. [(18)F]AIF-NOTA-FAPI-04 PET/CT uptake in metastatic lesions on PET/CT imaging might distinguish different pathological types of lung cancer. *Eur J Nucl Med Mol Imaging*. 2022;49:1671–81. <https://doi.org/10.1007/s00259-021-05638-z>.
 22. Thuillier P, Maajem M, Schick U, Blanc-Beguín F, Hennebicq S, Metges JP, et al. Clinical Assessment of 177Lu-DOTATATE quantification by comparison of SUV-based parameters measured on both post-PRRT SPECT/CT and 68Ga-DOTATOC PET/CT in patients with neuroendocrine tumors: a feasibility study. *Clin Nucl Med*. 2021;46:111–8. <https://doi.org/10.1097/rlu.0000000000003412>.
 23. Hu X, Zhou T, Ren J, Duan J, Wu H, Liu X, et al. Response prediction using (18)F-FAPI-04 PET/CT in patients with esophageal squamous cell carcinoma treated with concurrent chemoradiotherapy. *J Nucl Med*. 2022. <https://doi.org/10.2967/jnumed.122.264638>.
 24. Ren B, Cui M, Yang G, Wang H, Feng M, You L, et al. Tumor microenvironment participates in metastasis of pancreatic cancer. *Mol Cancer*. 2018;17:108. <https://doi.org/10.1186/s12943-018-0858-1>.
 25. Melucci AD, Chacon AC, Burchard PR, Tsagkalidis V, Casabianca AS, Goyal S, et al. The impact of carbohydrate antigen 19–9 on survival in patients with clinical stage I and II pancreatic cancer. *Ann Surg Oncol*. 2022;29:8536–47. <https://doi.org/10.1245/s10434-022-12497-x>.
 26. Halm U, Schumann T, Schiefke I, Witzigmann H, Mössner J, Keim V. Decrease of CA 19–9 during chemotherapy with gemcitabine predicts survival time in patients with advanced pancreatic cancer. *Br J Cancer*. 2000;82:1013–6. <https://doi.org/10.1054/bjoc.1999.1035>.
 27. Shi M, Yu DH, Chen Y, Zhao CY, Zhang J, Liu QH, et al. Expression of fibroblast activation protein in human pancreatic adenocarcinoma and its clinicopathological significance. *World J Gastroenterol*. 2012;18:840–6. <https://doi.org/10.3748/wjg.v18.i8.840>.
 28. MacNeil T, Vathiotis IA, Shafi S, Aung TN, Zugazagoitia J, Gruver AM, et al. Multiplex quantitative analysis of tumor-infiltrating lymphocytes, cancer-associated fibroblasts, and CD200 in pancreatic cancer. *Cancers*. 2021;13. <https://doi.org/10.3390/cancers13215501>.
 29. Kaghazchi F, Divband G, Amini H, Adinehpour Z, Akbarian AR. 68 Ga-FAPI-46 and 18 F-FDG in advanced metastatic pancreatic cancer. *Clin Nucl Med*. 2022;47:e666–9. <https://doi.org/10.1097/RLU.0000000000004316>.
 30. Zhang Z, Jia G, Pan G, Cao K, Yang Q, Meng H, et al. Comparison of the diagnostic efficacy of (68) Ga-FAPI-04 PET/MR and (18)F-FDG PET/CT in patients with pancreatic cancer. *Eur J Nucl Med Mol Imaging*. 2022;49:2877–88. <https://doi.org/10.1007/s00259-022-05729-5>.
 31. McBride WJ, Sharkey RM, Karacay H, D'Souza CA, Rossi EA, Laverman P, et al. A novel method of 18F radiolabeling for PET. *J Nucl Med*. 2009;50:991–8. <https://doi.org/10.2967/jnumed.108.060418>.
 32. D'Souza CA, McBride WJ, Sharkey RM, Todaro LJ, Goldenberg DM. High-yielding aqueous 18F-labeling of peptides via Al18F chelation. *Bioconjug Chem*. 2011;22:1793–803. <https://doi.org/10.1021/bc200175c>.
 33. Mona CE, Benz MR, Hikmat F, Grogan TR, Lueckerath K, Razmaria A, et al. Correlation of (68)Ga-FAPI-46 PET biodistribution with FAP expression by immunohistochemistry in patients with solid cancers: a prospective translational exploratory study. *J Nucl Med*. 2021. <https://doi.org/10.2967/jnumed.121.262426>.
 34. Connor AA, Gallinger S. Pancreatic cancer evolution and heterogeneity: integrating omics and clinical data. *Nat Rev Cancer*. 2022;22:131–42. <https://doi.org/10.1038/s41568-021-00418-1>.
 35. Wikberg ML, Edin S, Lundberg IV, Van Guelpen B, Dahlin AM, Rutegård J, et al. High intratumoral expression of fibroblast activation protein (FAP) in colon cancer is associated with poorer patient prognosis. *Tumour Biol*. 2013;34:1013–20. <https://doi.org/10.1007/s13277-012-0638-2>.
 36. Friemel J, Rechsteiner M, Frick L, Böhm F, Struckmann K, Egger M, et al. Intratumor heterogeneity in hepatocellular carcinoma. *Clin Cancer Res*. 2015;21:1951–61. <https://doi.org/10.1158/1078-0432.Ccr-14-0122>.
 37. Oramas DM, Moran CA. Thymoma: challenges and pitfalls in biopsy interpretation. *Adv Anat Pathol*. 2021;28:291–7. <https://doi.org/10.1097/pap.0000000000000310>.
 38. Mona CE, Benz MR, Hikmat F, Grogan TR, Lueckerath K, Razmaria A, et al. Correlation of (68)Ga-FAPI-46 PET Biodistribution with FAP expression by immunohistochemistry in patients with solid cancers: interim analysis of a prospective translational exploratory study. *J Nucl Med*. 2022;63:1021–6. <https://doi.org/10.2967/jnumed.121.262426>.
 39. Troost EG, Bussink J, Slootweg PJ, Peeters WJ, Merks MA, van der Kogel AJ, et al. Histopathologic validation of 3'-deoxy-3'-18F-fluorothymidine PET in squamous cell carcinoma of the oral cavity. *J Nucl Med*. 2010;51:713–9. <https://doi.org/10.2967/jnumed.109.071910>.
 40. Kaps L, Schuppan D. Targeting cancer associated fibroblasts in liver fibrosis and liver cancer using nanocarriers. *Cells*. 2020;9. <https://doi.org/10.3390/cells9092027>.
 41. Klinkhammer BM, Floege J, Boor P. PDGF in organ fibrosis. *Mol Aspects Med*. 2018;62:44–62. <https://doi.org/10.1016/j.mam.2017.11.008>.
 42. Kuburich NA, den Hollander P, Pietz JT, Mani SA. Vimentin and cytokeratin: good alone, bad together. *Semin Cancer Biol*. 2022;86:816–26. <https://doi.org/10.1016/j.semcancer.2021.12.006>.
 43. D'Ambrosi N, Milani M, Apolloni S. S100A4 in the physiology and pathology of the central and peripheral nervous system. *Cells*. 2021;10. <https://doi.org/10.3390/cells10040798>.
 44. Li Z, Li Y, Liu S, Qin Z. Extracellular S100A4 as a key player in fibrotic diseases. *J Cell Mol Med*. 2020;24:5973–83. <https://doi.org/10.1111/jcmm.15259>.
 45. Ding J, Qiu J, Hao Z, Huang H, Liu Q, Liu W, et al. Prognostic value of preoperative [(68) Ga]Ga-FAPI-04 PET/CT in patients with resectable pancreatic ductal adenocarcinoma in correlation with immunohistological characteristics. *Eur J Nucl Med Mol Imaging*. 2023. <https://doi.org/10.1007/s00259-022-06100-4>.
 46. Lee SM, Kim TS, Lee JW, Kim SK, Park SJ, Han SS. Improved prognostic value of standardized uptake value corrected for blood glucose level in pancreatic cancer using F-18 FDG PET. *Clin Nucl Med*. 2011;36:331–6. <https://doi.org/10.1097/RLU.0b013e31820a9ee4>.
 47. Xu HX, Chen T, Wang WQ, Wu CT, Liu C, Long J, et al. Metabolic tumour burden assessed by (1)(8)F-FDG PET/CT associated

- with serum CA19-9 predicts pancreatic cancer outcome after resection. *Eur J Nucl Med Mol Imaging*. 2014;41:1093–102. <https://doi.org/10.1007/s00259-014-2688-8>.
48. Goldstein D, El-Maraghi RH, Hammel P, Heinemann V, Kunzmann V, Sastre J, et al. nab-Paclitaxel plus gemcitabine for metastatic pancreatic cancer: long-term survival from a phase III trial. *J Natl Cancer Inst*. 2015;107. <https://doi.org/10.1093/jnci/dju413>.
 49. Kuten J, Levine C, Shamni O, Pelles S, Wolf I, Lahat G, et al. Head-to-head comparison of [(68)Ga]Ga-FAPI-04 and [(18)F]-FDG PET/CT in evaluating the extent of disease in gastric adenocarcinoma. *Eur J Nucl Med Mol Imaging*. 2021. <https://doi.org/10.1007/s00259-021-05494-x>.
 50. Koom WS, Seong J, Kim YB, Pyun HO, Song SY. CA 19–9 as a predictor for response and survival in advanced pancreatic cancer patients treated with chemoradiotherapy. *Int J Radiat Oncol Biol Phys*. 2009;73:1148–54. <https://doi.org/10.1016/j.ijrobp.2008.06.1483>.
 51. Rocha Lima CM, Savarese D, Bruckner H, Dudek A, Eckardt J, Hainsworth J, et al. Irinotecan plus gemcitabine induces both radiographic and CA 19–9 tumor marker responses in patients with previously untreated advanced pancreatic cancer. *J Clin Oncol*. 2002;20:1182–91. <https://doi.org/10.1200/jco.2002.20.5.1182>.
 52. Zhao L, Pang Y, Chen S, Chen J, Li Y, Yu Y, et al. Prognostic value of fibroblast activation protein expressing tumor volume calculated from [(68) Ga]Ga-FAPI PET/CT in patients with esophageal squamous cell carcinoma. *Eur J Nucl Med Mol Imaging*. 2023;50:593–601. <https://doi.org/10.1007/s00259-022-05989-1>.
 53. Fagerland MW. t-tests, non-parametric tests, and large studies—a paradox of statistical practice? *BMC Med Res Methodol*. 2012;12:78. <https://doi.org/10.1186/1471-2288-12-78>.
 54. Altman DG, Bland JM. Parametric v non-parametric methods for data analysis. *BMJ (Clinical research ed)*. 2009;338:a3167. <https://doi.org/10.1136/bmj.a3167>.
 55. Cui H, Guan J, Deng G, Yuan J, Lou C, Zhang W, et al. A Chinese retrospective multicenter study of first-line chemotherapy for advanced pancreatic cancer. *Med Sci Monit*. 2020;26:e927654. <https://doi.org/10.12659/MSM.927654>.

Publisher's note Springer Nature remains neutral with regard to jurisdictional claims in published maps and institutional affiliations.

Springer Nature or its licensor (e.g. a society or other partner) holds exclusive rights to this article under a publishing agreement with the author(s) or other rightsholder(s); author self-archiving of the accepted manuscript version of this article is solely governed by the terms of such publishing agreement and applicable law.

Authors and Affiliations

Ziyuan Zhu^{1,2} · Kai Cheng^{2,3} · Zhang Yun² · Xiang Zhang² · Xiaoyu Hu² · Jing Liu² · Fuhao Wang¹ · Zheng Fu^{2,3} · Jinbo Yue^{1,2}

Ziyuan Zhu
zhuzy158666@163.com

Kai Cheng
kcsdut@163.com

¹ School of Clinical Medicine, Weifang Medical University, Weifang, China

² Department of Radiation Oncology, Shandong Cancer Hospital and Institute, Shandong First Medical University and Shandong Academy of Medical Sciences, Jiyuan Road 440, Jinan, Shandong, China

³ PET/CT Center, Shandong Cancer Hospital and Institute, Shandong First Medical University, Shandong Academy of Medical Sciences, Jinan, Shandong, China